RSC Advances

PAPER

View Article Online
View Journal | View Issue

Cite this: *RSC Adv.*, 2021, **11**, 15512

Plant-based CO_2 drawdown and storage as SiC†

Suzanne T. Thomas, [a] Yongsoon Shin, [b] James J. La Clair [a] and Joseph P. Noel *[a]

Received 4th February 2021
Accepted 12th April 2021

DOI: 10.1039/d1ra00954k

rsc.li/rsc-advances

Since the 1950's the Earth's natural carbon cycle has not sufficiently sequestrated excess atmospheric CO_2 contributed by human activities. CO_2 levels rose above 400 ppm in 2013 and are forecasted to exceed 500 ppm by 2070, a level last experienced during the Paleogene period 25–65 MYA. While humanity benefits from the extraction and combustion of carbon from Earth's crust, we have overlooked the impact on global climate change. Here, we present a strategy to mine atmospheric carbon to mitigate CO_2 emissions and create economically lucrative green products. We employ an artificial carbon cycle where agricultural plants capture CO_2 and the carbon is transformed into silicon carbide (SiC), a valuable commercial material. By carefully quantifying the process we show that 14% of plant-sequestered carbon is stored as SiC and estimate the scale needed for this process to have a global impact.

Introduction

Earth rhythmically regulates the level of CO_2 wherein CO_2 transits between organic and inorganic carbon reservoirs (Fig. 1).[1] These exchanges occur in terrestrial, coastal, and deep marine ecosystems where carbon-rich biomass accumulates during photosynthesis. In turn, photosynthesis serves as a key biological process for establishing the global food chain while drawing down atmospheric CO_2 and sequestering carbon over wide time scales.[2,3] The majority of this CO_2-derived carbon is stored in minerals or as almost pure C in fossil fuels.[4] However, exponentially rising atmospheric levels of CO_2, positively correlated with economic development and the burning of fossil fuels, demonstrate that excess atmospheric carbon cannot be adequately mitigated by Earth's natural carbon cycles.[5–7] In fact, humanity has upset earth's CO_2 balance by releasing naturally recalcitrant carbon as CO_2 and methane, exemplified by liberation of 4 molecules of CO_2 per molecule of cement ($4\ CaO{\cdot}Al_2O{\cdot}Fe_2O_3$) manufactured from limestone ($CaCO_3$).[8]

Interestingly, Keeling curves[6,7] highlight the seasonal fluctuation in CO_2 levels due to photosynthetic activity and biomass decay.[9] In some regions, CO_2 concentrations fall by upwards of 20+ ppm over a growing season.[10] Food crops, however, only account for short-term sequestration since most are annually-grown, herbaceous plants that release their carbon reservoirs upon consumption or decomposition. Trapping unused plant carbon in a stable material, resistant to decomposition, would support mitigation of this seasonal re-release, possibly contribute to reducing atmospheric CO_2 through CO_2-based recycling, and enhance the economic value of repurposed CO_2 (left, Fig. 1).[2,11–13]

While stabilization of carbon cycles disrupted by anthropogenic emissions is a widely-appreciated necessity, CO_2 sequestration strategies[14,15] such as geological carbon storage only serve as stopgap solutions as they lack the permanent sinks required to prevent readmission to the atmosphere over short to intermediate time scales.

The ability of plants to utilize CO_2 as the central carbon source establishes their pivotal position as a biological sink in Earth's overall carbon balance, avoiding energy intensive direct air capture strategies, while affording facile methods to accurately quantify their net effect on atmospheric CO_2 levels when transformed into dense carbon-rich raw material. As such, plants generally provide a mitigating factor for CO_2 drawdown if properly utilized and their net contribution to synthetic carbon cycles quantified.[16] However, the predictive quantification of plant biomass transformation into recalcitrant forms of carbon are sorely lacking.[17,18]

Plant vegetation, including wood and rice husks, has been successfully transformed into a recalcitrant and commercially valuable form of carbon, namely silicon carbide (SiC).[19–21] SiC, due to its extreme strength, thermal stability, thermal conductivity, low weight, optical transparency, wide band gap, and inertness, make it highly profitable for applications in abrasive, defense, space, construction, solar, high temperature-high power electronics industries[22] and as a novel support for catalysis,[23,24] factors represented by recent, strong market growth. However, SiC is rarely found in nature; rather, it is produced synthetically from SiO_2, acid treatment, and petroleum coke

[a]*Jack H. Skirball Center for Chemical Biology and Proteomics, Salk Institute for Biological Studies, La Jolla, CA, USA. E-mail: noel@salk.edu; jlaclair@salk.edu*

[b]*Materials Sciences Division, Pacific Northwest National Laboratory, 902 Battelle Boulevard, Richland, WA, USA*

† Electronic supplementary information (ESI) available: Fig. S1–S6 and Tables S1–S3 as a PDF file and supplementary calculations as an XLS file. See DOI: 10.1039/d1ra00954k

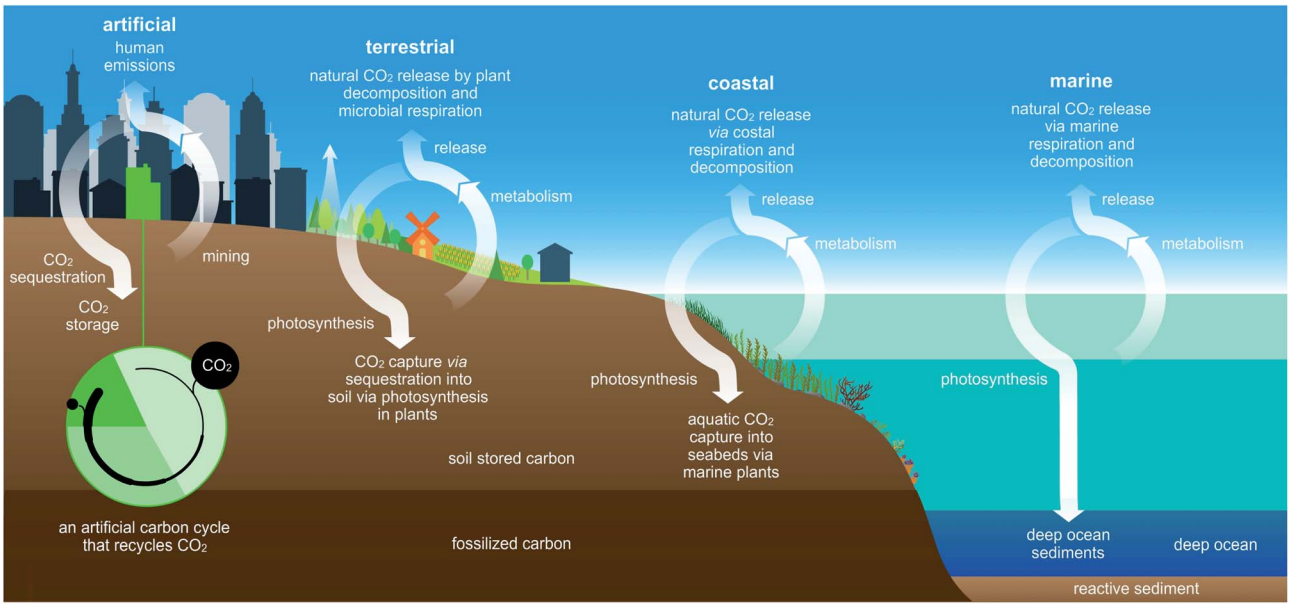

Fig. 1 Supplementing natural with artificial carbon cycles. Atmospheric CO_2 transits between the atmosphere and carbon-based mineral and liquid states in the Earth's crust. Terrestrial and aquatic plants play a key role by sequestering CO_2 from the atmosphere and storing it in sediments. In coastal and marine ecosystems, blue carbon is stored by mangroves, seagrasses (costal), macroalgae and phytoplankton (marine). While additional sequestration occurs through mineralization, photosynthesis plays a dominant short to intermediate term role in CO_2 capture and transformation. Since the industrial revolution, humanity has developed robust technologies to access stored carbon using processes that release CO_2 as a by-product thus upsetting the natural carbon balance. The development of artificial carbon cycles concentrated around industrialized centers (green building) could balance our planet's disrupted, natural carbon cycle through value-added recycling of atmospheric CO_2 into carbon-based materials.

(petcoke). Approximately 65% of C in petcoke is released into the atmosphere as CO_2 or methane during production.[25] Substituting petcoke with plant biomass during SiC production would potentially mitigate these carbon emissions, serve to recycle CO_2, and create value out of what is often considered an atmospheric pollutant if scalable and quantifiable methods are established.

Results and discussion

Here, we outline one quantitative strategy to reduce atmospheric CO_2 by recycling carbon through capture and storage cycles (Fig. 1), where plant biomass is petrified to synthesize SiC.[19–21] As illustrated in Fig. 2, this synthetic carbon cycle involves three processes: plant growth, plant processing, and biomass petrification. To explore the scale needed to make an impact on the atmosphere, we began with a short-lived, herbaceous crop, *Nicotiana tabacum*, cultivated tobacco.

We measured the net change in C content to quantify the efficiency of each step (Fig. 3 and 4). Tobacco seeds (Fig. 2) have an average mass of 70.5 ± 16.5 μg with 55.4 ± 14.2 mass% C when dry, amounting to $1.82 \pm 0.43 \times 10^{18}$ C atoms per seed (Fig. 4A and B). Seeds were planted and 58 days later leaves and stems harvested (Fig. 2). The resulting plant matter (Fig. 3A) was frozen, ground, and dried to a fine powder (Fig. 3B–E). The average "wet" plant mass was 34.9 ± 2.6 g and ~88 ± 2% of this "wet" mass consisted of water and other volatiles. The average dry plant mass was 4.2 ± 0.7 g (Table S1†). Eight dried plants

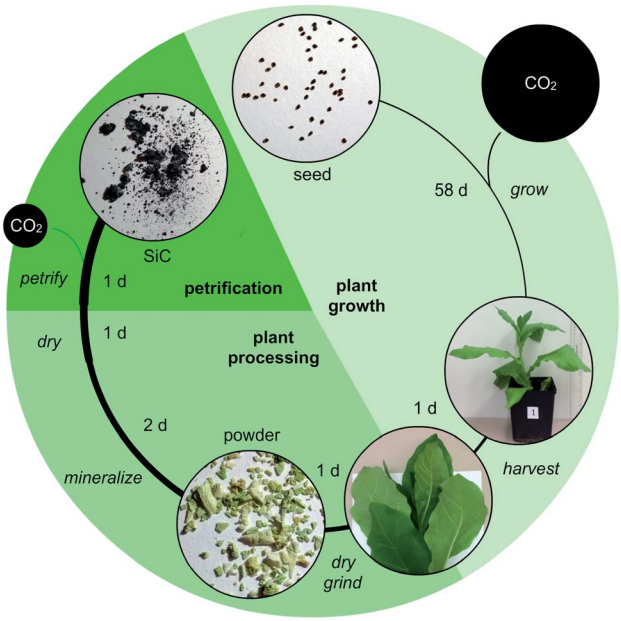

Fig. 2 An artificial carbon cycle producing SiC from plants. This cycle involves three processes: plant growth, plant processing, and biomass petrification comprised of six steps (grow, harvest, dry, grind, mineralize and petrify). The cycle begins with seeds and plant harvests 58 days later. Tissues are then frozen, ground, and dried to a fine powder. The resulting powders are then mineralized by treating with acid and perfusing by soaking in TEOS. Solutions were then air dried and subjected to combustion in inert atmospheres with heating and cooling regimens between room temperature and 1600 °C (see Methods).

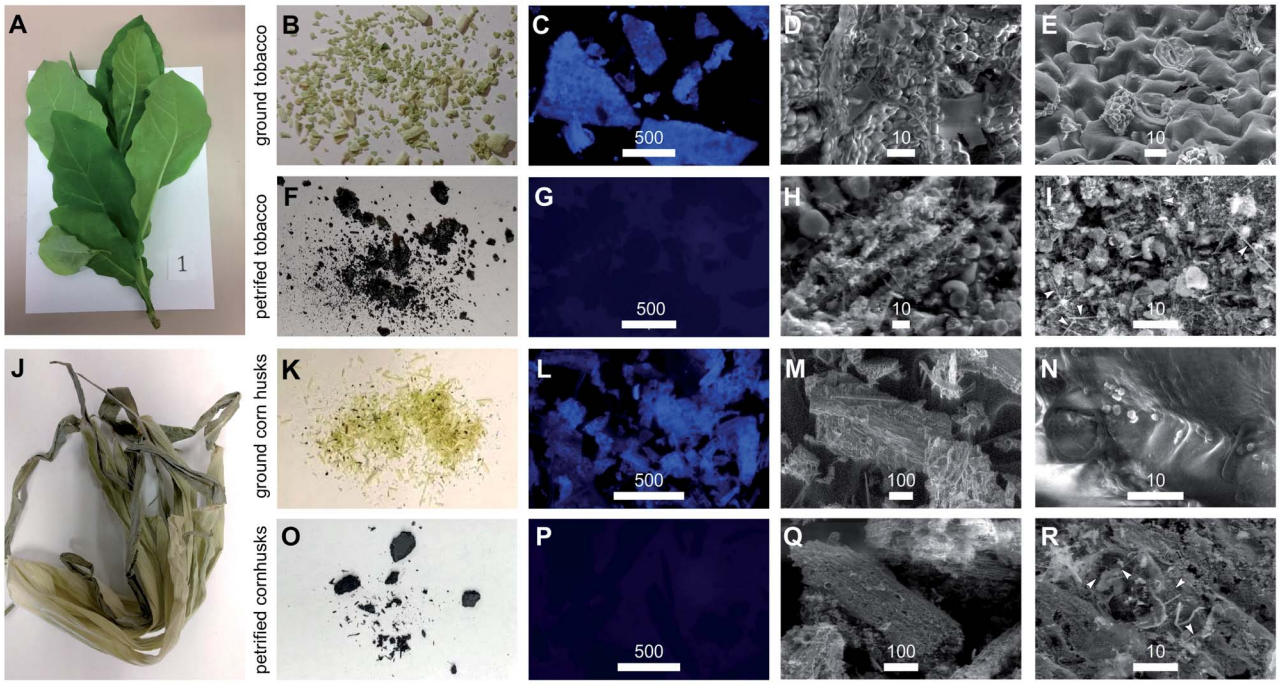

Fig. 3 Fresh and petrified tobacco and corn husks. (A) Photograph of the tobacco used in this study. (B–E) Representative images of ground tobacco tissue in (B), epifluorescence microscopy in (C), and SEM in (D and E). (F–I) Representative images of petrified tobacco products in (F), epifluorescence microscopy in (G), and SEM in (H and I). (J) Photograph of the corn husks used in this study. (K–N) Representative images of ground corn husks in (K), epifluorescence microscopy in (L), and SEM in (M and N). (O–R) Representative images of petrified corn husk products in (O), epifluorescence microscopy in (P), and SEM in (Q and R). Bars denote units in microns. The petrified products contain SiC whiskers coated with amorphous C as indicated by arrowheads.

were analyzed by energy dispersive X-ray spectroscopy (EDX) to quantify elemental composition. Dried plant powders on average contained 43.7 ± 2.0 mass% C per plant, amounting to 1.8 ± 0.4 g of C or 9.2 ± 1.8 × 10^{22} C atoms per tobacco plant (Fig. 4A, B and Table S1†). The net change in C content from seed to plant was a positive gain of 1.8 ± 0.4 g of C or 9.2 ± 1.8 × 10^{22} C atoms per tobacco plant removed from the atmosphere and converted into biomass. Overall, this equates to a 50 000-fold increase in biologically sequestered carbon from seed to plant in 58 days under standard laboratory growth conditions.

Duplicate samples of dried tobacco powder (0.65–0.90 g) from each plant (Fig. 3B and Table S1†) were mineralized by acidic disruption followed by soaking in tetraethyl orthosilicate (TEOS) and petrified by combustion in an alumina tube furnace at temperatures reaching 1600 °C. Over multiple runs, we obtained a greenish gray to dark gray material (Fig. 3F). We used X-ray diffraction (XRD) to analyze the structural composition of the petrified products (Fig. 5).[19,20] The major component in all samples was β-SiC.[19–21] Amorphous C was also evident in the broad XRD peak centered at 26°. The amount of pure C varied across samples due to variability in the efficiency of the mineralization step. Diffraction peaks characteristic of SiO_2 were not observed consistent with the mineralization reaction proceeding to completion with SiO_2 being the limiting reactant.

Samples of the initial plant powders and petrified products were evaluated using a combination of epifluorescence microscopy and scanning electron microscopy (SEM). Using 357 ± 44 nm excitation and 447 ± 60 nm emission to monitor chlorophyll autofluorescence, complete losses of 447 nm emissions upon petrification were observed as illustrated by

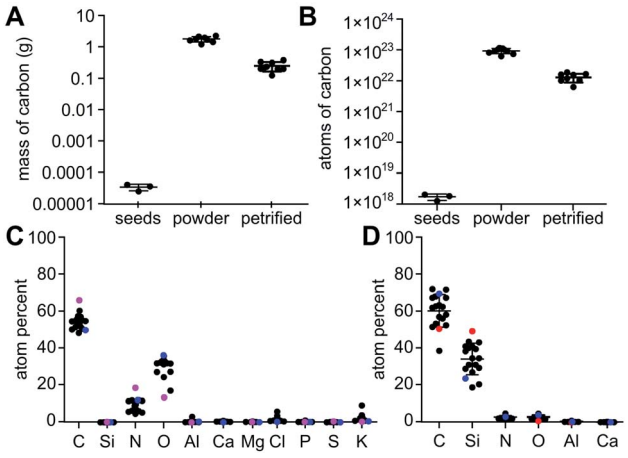

Fig. 4 Characterization of tobacco plants and petrified tobacco products. (A) Mass of C per tobacco seed, powdered tobacco plant material, and petrified tobacco samples calculated from sample weight and the % mass of C detected by EDX analyses. (B) Atoms of C per tobacco seed, powdered tobacco plant material, and petrified tobacco samples calculated using the mass of C from (A). (C) Elemental composition of starting plants and (D) petrified product samples by EDX. Tobacco plants shown in black, seeds shown in purple, corn husks shown in blue, and SiC standard shown in red.

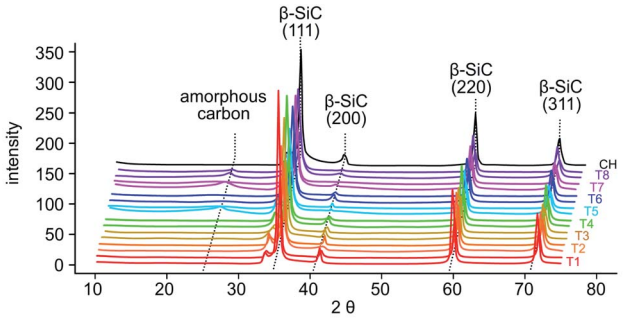

Fig. 5 XRD spectra of samples of the petrified tobacco products (T1–T8, colored) in duplicate and corn husks (CH, black).

comparison of Fig. 3C–G. Using SEM, we consistently preserved cellular structures within the plant tissue (Fig. 3D, E, S1 and S2†) during mineralization and petrification (Fig. 3H, I and S3†). SEM also revealed the formation of SiC whiskers coated with amorphous C (arrows, Fig. 3I).[19,20] In total, these microscopic features may someday translate into using plants to manufacture nanometer scale carbon catalysts, catalyst supports and SiC devices.[21,22]

Multiple EDX measurements focused on different positions across each sample identified and quantified Si, C, O, and N plus trace components (Fig. S6†). The major elements found in tobacco seeds by EDX include C, N, and O at 66.4 ± 6.8, 18.6 ± 4.8, and 13.7 ± 4.6 atom%, respectively (Fig. 4C and Table S2†). Tobacco plants used for the petrification process on average contained C, O, and N at 53.7 ± 3.2, 31.7 ± 2.9 and 8.6 ± 2.7 atom%, respectively (Fig. 4C and Table S2†). The minor elements K and Cl and the trace elements Al, Ca, Mg, Cl, P, S, and Si were also observed at <2.5% and <1%, respectively, in tobacco plants and seeds.

In the petrified products, average amounts of Si and C measured by EDX were 33.9 ± 7.8 atom% and 60.6 ± 7.2 atom%, respectively (Fig. 4D and Table S3†). The higher level of C was consistent with the XRD-based detection of amorphous C. The variability in Si to C ratios amongst samples is likely due to the heterogeneity of the SiC product and varied across locations used for EDX data acquisition. Ratios near one were obtained for some samples, 43.3 ± 11.1 atom% Si and 51.2 ± 9.0 atom% C. These near stoichiometric ratios are in line with commercially available SiC powders exhibiting 48.9 ± 15.1 atom% Si and 50.2 ± 15.0 atom% C on average (Fig. 4D and Table S3†). The petrified material contained only minor impurities including <3% N and O and <1% Al and Ca while Mg, Cl, P, S, and K were below detectable limits (Fig. 5 and Table S3†). The largest impurity detected, pure C, was evident from the less than stoichiometric ratio of Si to C. As impurities in SiC hinder crystallization and wafer production required for high-end applications in electronics, optimization efforts, higher temperatures and/or application of established purification methods will be required.[19,20,26]

Overall, we achieved a net gain of sequestered C, 0.26 ± 0.09 g of C or 1.28 ± 0.43 × 10^{22} atoms of C per tobacco plant, from the atmosphere and stored it as SiC with minimal amounts of amorphous C. The net percentage of C retained was 13.8 ± 2.9% averaged over 16 samples (Table S1†). From studies on wood, mass loss upon heating to 500 °C is unavoidable, as pyrolytic decomposition of hemicellulose, cellulose and lignin results in the release of H_2O, CO_2, and volatile hydrocarbons.[20]

We next explored a second plant material, corn husks, that represent by-products of a current agricultural crop that would avoid large scale changes in land use to implement. Using a similar procedure (Fig. 2), we prepared powder from ground and dried husks (Fig. 3J–N and S4†) and subjected the resultant materials to petrification yielding black powders (Fig. 3O–R and S5†). Epifluorescence was completely lost from plant material (Fig. 3L) to petrified product (Fig. 3P). In short, remarkable preservation of the tissue structures occurred after three-step processing (Fig. 3M, N and S4† *versus* Fig. 3Q, R and S5†). The most abundant elements found in petrified corn husks measured by EDX were comparable to amounts obtained for petrified tobacco with Si, C, O and N at 23.5 ± 3.6, 69.1 ± 2.8, 3.9 ± 0.9, and 3.1 ± 0.7 atom%, respectively (Table S3†). The overall percentage of C retained through this process was 14.3% indicating that this procedure is amenable to carbon capture and SiC production using agricultural by-products that normally release almost their entire stockpile of carbon in the form of CO_2 and methane (Table S1†).

We calculated the production of 1.8 g of SiC (total of the petrified mass in Table S2†) required an estimated 177 kW h, including energy required for instrumentation and estimated energy for reagent preparation. The majority, 125 kW h, was used to power the furnace in the petrification step with the remaining 52 kW h spent on heating, vacuum drying and reagents associated with the mineralization step.

Ongoing quantitative work is focused on identifying plant tissues and biomolecules resistant to loss of CO_2 during heating, increasing the efficiency of the overall retention of biological C, use of renewable energies, and demonstration of scalability. Presently, this method would require each person on earth to plant, harvest, and dry the equivalent of 450 to 5000 tobacco plants to sequester 1 gigaton (Gt) of CO_2, based upon measurements of tobacco plant mass used for biofuels and smoking industries, respectively (ESI calculations†).

While not carbon-neutral, this process represents a laboratory scale model in which energy consumption was not optimized. Based on the US EPA AVERT emission factor of 7.07 × 10^{-4} metric tons of CO_2 per kW h,[27] the energy requirements for this process (177 kW h) would have released 0.125 metric tons (125 kg) of CO_2. With advances in recycling of agricultural waste streams, solar concentration systems (HelioHeat, Heligen Corp.), radiofrequency (inductive) heating, the storage of heat using molten salts,[28] and efficient use of alternative sources of energy,[29] the high temperatures used in this process should scale and approach neutrality in their overall C footprint. For instance, the solar furnace located in Font-Romeu-Odeillo-Via routinely reaches temperatures exceeding 3500 °C in a matter of seconds using a series of mirrors to focus a large amount of sunlight.[30] Additionally, identifying plants with sufficient levels of endogenous SiO_2 could eliminate the mineralization step (acid treatment and perfusion with TEOS) contributing to the

economic value of SiC by enhancing purity.[20] Grasses and waste products from rice already contain high SiO_2 levels.[31] Finally, identification of plant species and varieties harboring densely packed, carbon-rich biomolecules such as suberin that are more quantitatively converted to SiC without losses due to pyrolytic decomposition should substantially increase the net gain of sequestered C per plant.

Conclusions

Harnessing plants to absorb and transform CO_2 may lead to mobilization of plants to generate C-friendly, green components for consumer goods, electronics and advanced materials. Together with complementary technologies such as biochar production,[32] SiC manufacturing can positively contribute to future rectification of the imbalance in atmospheric CO_2 contributing to global climate change. Here, we precisely quantify the carbon capture potential of an artificial carbon cycle that draws down CO_2 from the atmosphere in rapidly growing agricultural plants and then stores C atoms permanently in SiC, a rare mineral in nature with increasing demand in the electronics, automotive, defense, construction, space, energy and abrasive industries. While additional purification steps[33,34] would need to be implemented before such applications could be achieved, this method suggests a natural alternative to source SiC.[35]

This system offers a tractable means to monitor CO_2 draw down and provides an opportunity for replicating the microstructure and morphology of a unique array of starting materials to fabricate novel SiC architectures. This idea is complementary to ongoing efforts to develop biomorphic cellular SiC ceramics from plant materials, including a variety of woods[20,36–40] and agricultural products, broomcorn millet[41] and cotton stalks.[41] Adaptation of the molding processes allows the direct shaping of the final material and generates SiO *in situ*, which promotes conversion of residual carbon into SiC.[42]

Overall, this study demonstrates how integration of plants into an artificial carbon cycle is capable of harmoniously operating with Earth's natural carbon cycles (Fig. 1) as one means to recycle atmospheric CO_2 for economically lucrative green materials.[43]

Materials and methods

Plant material

N. tabacum cv. Xanthi plants were grown under artificial light with 16 h light periods and harvested 58 days from when seeds were planted. Cornhusks were obtained from Sprouts Farmers Market, San Diego. *N. tabacum* seeds, plant stems and leaves, and corn husks were frozen in liquid nitrogen, ground by mortar and pestle, and dried by lyophilization.

Mineralization

Samples ranging from 0.2703 g to 0.9179 g were soaked in 30 mL of 2 M HCl at 60 °C for 24 h. The solution was removed and dried under vacuum at 60 °C. Each dried sample was perfused with 23 mL solutions of TEOS (5.0 g), 2 M HCl (2.5 mL), EtOH (10 mL) and H_2O (5.0 mL) with a molar ratio = 1.000 : 20.80 : 71.40 : 173.4, respectively, and kept at 60 °C for 16 h. Processing was done in triplicate.

Petrification

Solids were separated from the solutions, air-dried, placed in alumina boats and set in a horizontal alumina tube furnace. Combustion was carried out in an inert argon atmosphere warming from 23 °C to 1000 °C at 5 °C min^{-1}, 1000–1600 °C at 3 °C min^{-1}, heating at 1600 °C for 2 h then cooling from 1600–1000 °C at 2 °C min^{-1}, 1000–300 °C at 3 °C min^{-1}, and 300–23 °C at 5 °C min^{-1}. Multiple runs generated greenish gray to dark gray powders.

Characterization

X-ray diffraction (XRD) patterns were obtained on a desktop X-ray diffractometer (Rigaku) using Cu Kα (1.54059 Å) radiation with the X-ray generator operating at 20 kV and 30 mA. Data were collected for 2θ range of 10.0–75.0° at an angular resolution of 0.01° s^{-1}. SEM images and elemental microanalysis were acquired on a FEI Quanta FEG 250 scanning electron microscope equipped with an energy dispersive spectrometer operating at 10 kV and 1.5–2 mbar for five or more points per sample. Epifluorescence images were collected on an EVOS FL (Invitrogen) imaging system using 357 ± 44 nm excitation and 447 ± 60 nm emission to monitor chlorophyll autofluorescence.

Author contributions

S. T. T. grew plants. S. T. T. and J. J. L. harvested, dried, and ground plant samples. S. T. T. and J. J. L. prepared samples for combustion, SEM, and EDX analyses. S. T. T. and J. J. L. conducted the fluorescent imaging. S. T. T., J. J. L., and J. P. N. evaluated imaging and elemental analyses data. Y. S. conducted drying, petrification, and XRD analyses. S. T. T., J. J. L., and J. P. N. developed the project and interpreted the results. All authors contributed to the writing.

Conflicts of interest

There are no conflicts to declare.

Acknowledgements

This research was supported by the National Science Foundation (Grant No. EEC-0813570) through the Engineering Research Center CBiRC (Center for Biorenewable Chemicals). A portion of the research was funded by the Howard Hughes Medical Institute and performed at Pacific Northwest National Laboratory (PNNL), operated by Battelle Memorial Institute for the U.S. DOE under contract DE-AC 06-76RLO 1830, using the Agreements for Commercializing Technology (ACT) program. We thank the Nano3 facility at UC San Diego for conducting the SEM and EDX spectroscopy studies and Nina Seiler for assistance with the preparation of Fig. 1.

Notes and references

1 P. Falkowski, *et al.*, The global carbon cycle: a test of our knowledge of earth as a system, *Science*, 2000, **290**, 291–296.
2 D. Bonaventura, *et al.*, Dry carbonate process for CO_2 capture and storage: integration with solar thermal power, *Renewable Sustainable Energy Rev.*, 2018, **82**, 1796–1812.
3 D. Baldocchi, Y. Ryu and T. Keenan, Terrestrial carbon cycle variability, *F1000Research*, 2016, **5**, 2371.
4 R. M. Hazen, D. R. Hummer, G. Hystad, R. T. Downs and J. J. Golden, Carbon mineral ecology: predicting the undiscovered minerals of carbon, *Am. Mineral.*, 2016, **101**, 889–906.
5 R. Monastersky, Global carbon dioxide levels near worrisome milestone, *Nature*, 2013, **497**, 13–14.
6 D. E. Pataki, *et al.*, The application and interpretation of Keeling plots in terrestrial carbon cycle research, *Global Biogeochem. Cycles*, 2003, **17**, 1022.
7 C. D. Keeling, Rewards and penalties of monitoring the Earth, *Annu. Rev. Energy Environ.*, 1998, **23**, 25–82.
8 L. Shen, T. Gao, J. Zhao and L. Wang, Factory-level measurements on CO_2 emission factors of cement production in China, *Renewable Sustainable Energy Rev.*, 2014, **34**, 337–349.
9 A. Eldering, *et al.*, The Orbiting Carbon Observatory-2 early science investigations of regional carbon dioxide fluxes, *Science*, 2017, **358**, eaam5745.
10 https://www.esrl.noaa.gov/gmd/ccgg/carbontracker/.
11 W. Ampomah, *et al.*, Optimum design of CO_2 storage and oil recovery under geological uncertainty, *Appl. Energy*, 2017, **195**, 80–92.
12 Y. Zhu, C. Romain and C. K. Williams, Sustainable polymers from renewable resources, *Nature*, 2016, **540**, 354–362.
13 A. Goeppert, M. Czaun, J. P. Jones, G. K. S. Prakash and G. A. Olah, Recycling of carbon dioxide to methanol and derived products – closing the loop, *Chem. Soc. Rev.*, 2014, **43**, 7995–8048.
14 A. Mamoori Al, A. Krishnamurthy, A. A. Rownaghi and F. Rezaei, Carbon capture and utilization update, *Energy Technol.*, 2017, **5**, 834–849.
15 S. Nanda, S. N. Reddy, S. K. Mitra and J. A. Kozinski, The progressive routes for carbon capture and sequestration, *Energy Sci. Eng.*, 2016, **4**, 99–122.
16 P. Jajesniak, A. Hemo and T. S. Wong, Carbon dioxide capture and utilization using biological systems: opportunities and challenges, *J. Bioprocess. Biotech.*, 2014, **4**, 1–15.
17 Z. Gao, Y. Zhang, N. Song and X. Li, Biomass-derived renewable carbon materials for electrochemical energy storage, *Mater. Res. Lett.*, 2016, **5**, 69–88.
18 M.-M. Titirici and M. Antonietti, Chemistry and materials options of sustainable carbon materials made by hydrothermal carbonization, *Chem. Soc. Rev.*, 2010, **39**, 103–116.
19 Y. Shin, C. Wang and G. J. Exarhos, Synthesis of SiC ceramics by the carbothermal reduction of mineralized wood with silica, *Adv. Mater.*, 2005, **17**, 73–77.
20 P. Greil, Y. Lifka and A. Kaindl, Biomorphic cellular silicon carbide ceramics from wood: I. Processing and microstructure, *J. Eur. Ceram. Soc.*, 1998, **18**, 1961–1973.
21 Y. L. Chiew and K. Y. Cheong, A review on the synthesis of SiC from plant-based biomasses, *Mater. Sci. Eng., B*, 2011, **176**, 951–964.
22 R. Wu, K. Zhou, C. Y. Yue, J. Wei and Y. Pan, Recent progress in synthesis, properties and potential applications of SiC nanomaterials, *Prog. Mater. Sci.*, 2015, **72**, 1–60.
23 J. Sun, Q. Feng, Q. Liu, S. Ji, Y. Fang, X. Peng and Z.-J. Wang, Al_2O_3-coated SiC-supported Ni catalyst with enhanced activity and improved stability for production of synthetic natural gas, *Ind. Eng. Chem. Res.*, 2018, **57**, 14899–14909.
24 Y. Guo, Z. Zou, X. Shi, P. Rukundo and Z.-J. Wang, *ACS Sustainable Chem. Eng.*, 2017, **5**, 2330–2338.
25 *Technical support document for the Si carbide production sector: Proposed rule for mandatory reporting of greenhouse gases*, Office of Air and Radiation, U.S. Environmental Protection Agency, 2009.
26 F. Mao, D. Wu, Z. Zhou and S. Wang, Removal of amorphous carbon from SiC powder using flotation, *Sep. Sci. Technol.*, 2014, **49**, 792–796.
27 EPA, *AVERT, U.S. national weighted average CO_2 marginal emission rate, year 2018 data*, U.S. Environmental Protection Agency, Washington, DC, 2019.
28 G. Reddy, Molten salt thermal energy storage materials for solar power generation, *Ninth International Conference on Molten Slags, Fluxes and Salts (Molten 12)*, The Chinese Society for Metals, Beijing, China, CD, 2012, vol. 1–18.
29 A. Modi, F. Bühler, J. G. Andreasen and F. Haglind, A review of solar energy based heat and power generation systems, *Renewable Sustainable Energy Rev.*, 2017, **67**, 1047–1064.
30 G. Olalde and J. L. Peube, Etude expérimentale d"un récepteur solaire en nid d"abeilles pour le chauffage solaire des gaz à haute température, *Rev. Phys. Appl.*, 1982, **17**, 563–568.
31 B. S. Tubana, T. Babu and L. E. Datnoff, A review of silicon in soils and plants and its role in US agriculture: history and future perspectives, *Soil Sci.*, 2016, **181**, 393–411.
32 D. Woolf, J. E. Amonette, F. A. Street-Perrott, J. Lehmann and S. Joseph, Sustainable biochar to mitigate global climate change, *Nat. Commun.*, 2010, **1**, 56.
33 R. S. Evans, D. L. Bourdell, J. J. Beaman and M. I. Campbell, Rapid manufacturing of silicon carbide composites, *Rapid Prototyp. J.*, 2005, **11**, 37–40.
34 Y. M. Chiang, R. P. Messner, C. D. Terwilliger and D. R. Behrendt, Reaction-formed silicon-carbide, *Mater. Sci. Eng., A*, 1991, **144**, 63–74.
35 C. R. Eddy, Jr and D. K. Gaskill, Silicon Carbide as a Platform for Power Electronics, *Science*, 2009, **324**, 1398–1400.
36 P. Griel, T. Liftka and A. Kaindl, Biomorphic cellular silicon carbide ceramics from wood: II. Mechanical properties, *J. Eur. Ceram. Soc.*, 1988, **18**, 1975–1983.

37 A. Karim, A. Ghosh, R. Rao and M. Krishnan, Biomorphic SiC: porous SiC and ultrafine SiC powder formation through biomimicking route, *Adv. Appl. Ceram.*, 2021, **120**, 24–31.

38 M. Yu, G. Z. Zhang and T. Saunders, Wood-derived ultra-high temperature carbides and their composites: a review, *Ceram. Int.*, 2020, **46**, 5536–5547.

39 J. M. Qian, Z. H. Jin and X. W. Wang, Porous SiC ceramics fabricated by reactive infiltration of gaseous silicon into charcoal, *Ceram. Int.*, 2004, **30**, 947–951.

40 Q. Wang, Y. H. Zhang and Y. W. Guo, Biomorphic hierarchical porous SIC prepared from carbonized broomcorn millet, *Rare Met. Mater. Eng.*, 2015, **44**, 662–664.

41 Q. Wang, X. Cheng and Y. H. Zhang, Biomorphic h SIC prepared from cotton stalk, *Rare Met. Mater. Eng.*, 2013, **42**, 748–750.

42 P. Nguyen and C. Pham, Innovative porous SiC-based materials: from nanoscopic understandings to tunable carriers serving catalytic needs, *Appl. Catal., A*, 2011, **391**, 443–454.

43 T. Kuramoci, A. Ramirez, W. Turkenburg and A. A. Faaij, Comparative assessment of CO_2 capture technologies for C-intensive industrial processes, *Prog. Energy Combust. Sci.*, 2012, **38**, 87–112.